

# Agemo: an open-source library for Laplace transformed coalescence time distributions.

Gertjan Bisschop \*

Institute of Evolutionary Biology, University of Edinburgh, EH9 3FL Edinburgh,  
Scotland

## Abstract

We can only start to capture the stochasticity of the coalescent under a specified model once we consider the full (joint) distribution of total branch lengths. In turn extracting the distribution of meaningful statistics can be computationally challenging. The Laplace transform is a natural way of studying coalescence time distributions. This distribution can be generated by means of a simple set of recursive instructions irrespective of model complexity. The approach has previously been used to fit demographic models and estimate sweep parameters by calculating likelihoods for patterns of linked variants. Here we present agemo, an open-source tool to generate and efficiently query that distribution. We rely on the fact that its generating function can be represented most simply as a directed graph with all possible ancestral states of the sample as nodes. A graph traversal algorithm then allows us to efficiently evaluate the generating function. Particular attention is paid to the block-wis site frequency spectrum (bSFS). Not only can likelihoods be calculated more efficiently, the implementation is also more general by allowing users to take phase information into account. The work laid out here will make it possible to fit more complex demographic models and use more of the information available after sequencing.

---

\*g.bisschop@sms.ed.ac.uk

# 1 Introduction

Laplace transforms have been used extensively in coalescent theory since the introduction of the structured coalescent (Takahata, 1988; Notohara, 1990; Barton and Wilson, 1995). Initially it was a formal tool to analyse continuous-time Markov chains (Takahata, 1988; Griffiths, 1991; Wilkinson-Herbots, 1998). But as noted by Wilkinson-Herbots (1998), the Laplace transforms of the distributions of coalescence times are also interesting in their own right. The Laplace transform of a random variable has a clear probabilistic interpretation. One can think of that random variable as describing the length of an interval. If a Poisson marking process with intensity  $\omega$  marks the interval, then the Laplace transform  $f^*(\omega)$  is the probability of not observing any marks in the considered interval (Råde, 1972). Let the random variable be the stochastic process modelling the (sum of the) exponentially distributed waiting times describing the ancestry of a random sample, then the marking process can describe the arrival of mutations. Formulated as such, the connection to the coalescent (Kingman, 1982; Hudson, 1983; Tajima, 1983) becomes obvious, making the Laplace transform a natural choice (Weissman and Hallatschek, 2017).

Moreover, used in mathematical fields like queueing theory, the Laplace transform often provides us with an alternative description of the behaviour of a system, often simplifying its analysis in the process. In essence, this is what the generating function (GF) method as described in Lohse et al. (2011) does. Using the probabilistic interpretation of the Laplace and the fact that the transform turns convolution into multiplication (see 2.1), one can come up with a much simpler, recursive and automated, description of the distribution of the (sum of) inter-event times given a set of samples and a (structured coalescent) model. Phrased differently, being given a flow diagram or coalescent state space graph describing all possible transitions during the coalescent process (see fig. 2.1.2), one can readily write down all associated expressions in the Laplace domain. This is not the case for the time domain.

The GF framework has been used to tackle two major problems in population genetics: estimating sweep parameters (Bisschop et al., 2021) as well fitting explicit models of population history (Lohse et al., 2011; Bunnefeld et al., 2015; Lohse et al., 2016). To study the how fast populations diverge in the face of gene flow, a lot of focus has gone to isolation with migration type (IM) models (Nielsen and Wakeley, 2001). This class of models where two populations split off from an ancestral population at some point in the past and experience gene flow between them from that point onwards are simple yet informative. They allow us to study the impact of ongoing gene flow on the coalescent histories along the genome. It has been remarked before that the GF framework is general in the sense that most of the analytical results for specific instances of these types models are just special cases of the general solution provided by the GF (Lohse et al., 2016).

The ability to make mathematically tractable descriptions of a problem as well the ability to efficiently implement the solution are two bottlenecks that hold for all inference problems (in population genetics). The first issue is generally solved by making simplifying assumptions about recombination, either ignoring the information contained within closely linked variants completely (Gutenkunst et al., 2009; Excoffier et al., 2013), or by only ignoring recombination within very short blocks (Yang, 2002; Hey, 2004; Lohse et al., 2011). Additionally, because the state space of all possible events describing the coalescent history of a sample will grow super-exponentially with sample-size and the number of considered events, there will always be limitations to the sample size and/or the number of events for which a detailed description of the ancestral process can be generated and more importantly evaluated within reasonable (memory) space and time.

The second issue is often very closely connected to the type of mathematical description used. In general, one will benefit from the potential to implement a particular solution in terms of data structures for which efficient algorithms exist for each of the required basic operations. For example, preserving matrix structure up to the point of evaluation, as used in phase-type theory (Hobolth et al., 2019), will tend to have a positive impact on performance due to the existence of many efficient algorithms for linear algebra operations.

So far, all inference approaches using the GF, rely on deriving the probability of observing each of the different block-wise site frequency spectrum (bSFS) vectors. These combinations of mutation configurations along the distinguished branch types within blocks of a certain length summarise the joint distribution of linked polymorphisms (Bunnefeld et al., 2015). However, depending on both the number of observed mutations and the number of distinguished branch types, they require repeated differentiation of the entire GF. As a consequence, any naive implementation of the GF with higher-order derivatives using a computer algebra system (CAS) will quickly run into computational bottlenecks, essentially limiting the extendability of the framework.

Previous efforts to make the framework more efficient have targeted the first bottleneck category by limiting the number of distinguishable branch types, limiting the number of occurrences of particular events, and using symmetries within the recursive description (Lohse et al., 2016). No attempts have been made to tackle the second bottleneck and describe the problem in a way that allows for more efficient computation.

Here we present the first open-source implementation of the GF framework and lay out the key algorithms that allow us to efficiently calculate the bSFS by using the correspondence between the recursive formulation of the Laplace transform and the coalescent state space graph. The focus on the bSFS is only superficial however. Any future extension of the library will make use of the concepts outlined here.

First, we will outline how the GF can be represented more succinctly. Secondly, we will lay out

the graph traversal algorithm allowing us to efficiently evaluate the GF. We will then apply this to the bSFS by using the algorithm to propagate the coefficients of a truncated Taylor series through the graph. Finally, we show how to extend bSFS type calculations to the fully phased and rooted case by making use of mutation type symmetries to limit the amount of computation needed.

## 2 Methods

### 2.1 Recursive description of the Laplace transform

#### 2.1.1 single population

Given a sample of  $n$  uniquely labelled lineages  $\Omega = \{a, \dots, n\}$  coming from a single population, we can represent all possible coalescent histories of that sample as a series of trees. In each of these ranked topologies nodes represent the lineage ancestral to the subtended nodes. Alternatively, the same information can be captured by a single rooted directed graph describing the state space of all (coalescence) events affecting the history of the sampled lineages. In this graph, each node is uniquely labelled by one of the partitions of  $\Omega$ . As lineages coalesce, we move through the graph from the source node, representing the set of all sampled lineages, to the root or most recent common ancestor (mrca). In the case of the neutral coalescent and a single population each path through the graph is equivalent to a single ranked topology. However, in general the state space graph will contain information on all events that affect the lineage configuration, not only those that join to lineages.

For  $k$  uncoalesced lineages, the rate of coalescence is  $\binom{k}{2}$  (in units of  $2N_e$  generations). Because each step is conditionally independent of the previous and as touched upon in the introduction, the Laplace transform of the sum of inter-event times or the time to the most recent common ancestor ( $t_{mrca}$ ) is a simple product of all Laplace transforms of the random variable describing the waiting time to go from  $k$  to  $k-1$  lineages. As such, we can associate each edge of the directed graph with a single equation describing this transition. The Laplace transform of the  $t_{mrca}$  for a single (ranked) topology can then be retrieved by multiplying the equations associated with a single path of the graph. Likewise, the entire GF is the sum of all expressions retrieved by a depth-first traversal of the graph (see 2.1.2).

Knowing that the equation associated with a single edge in the coalescent state space graph as outlined above, gives the probability of observing the coalescence event prior to any other event happening at rate  $\omega$ , for any two out of  $k$  lineages, the Laplace transform is  $f^*(\omega) = \frac{1}{\binom{k}{2} + \omega}$ . Note that in general we can label each branch connecting two lineages in a coalescent tree by the samples that will be affected by a mutation arising during the time represented by that branch. And in

104 general, we will associated each of these branch types with a unique dummy variable. Replacing  $\omega$   
 105 by  $\sum_{i=1}^b \omega_i$ , we can retrieve the coalescence time distribution for each of the  $b$  distinguished branch  
 106 types (Lohse et al., 2011).

### 107 2.1.2 general form

108 So far, we have dealt with a single population, tracking only coalescence events. In a structured  
 109 population, we require at least one type of (migration) event to ensure lineages eventually all end  
 110 up in the same population to allow for coalescence. These events can be incorporated in the state  
 111 space graph by adding a node for each of these events and labelling that node by their impact on the  
 112 tracked set of lineages. Looking at any node in the graph, the set of all possible events is determined  
 113 by all outgoing edges and the set of all observable branchtypes during the time represented by each  
 114 edge will be given by the label of the node from which the edges are leaving. The LT associated  
 115 with a single edge still describes the probability of observing a particular event prior to all other  
 116 events. So as long as the events that we have added in are associated with exponentially distributed  
 117 waiting times and given that  $\min(X, Y) \sim \exp(\omega_1 + \omega_2)$  when both  $X \sim \exp(\omega_1)$  and  $Y \sim \exp(\omega_2)$ ,  
 118 we can still readily associate each edge with the correct equation.

$$f[\omega] = \frac{c}{\sum c_i \kappa_i + \sum l_j \lambda_j + \sum o_k \omega_k} \quad (1)$$

119 Here, Roman letters represent integers counting the number of ways a certain (coalescence or  
 120 other) event can take place ( $c_i, l_j$ ) given the current state space, or the number of branches of a  
 121 particular type ( $o_i$ ). The Greek letters represent the rate of the associated competing processes.  
 122 Note that in the case of coalescence with multiple populations, rates are relative and given by  
 123  $\kappa_i = N_{e_i} / N_{ref}$ .

124 Each equation can be encoded as a matrix with two rows containing the integer coefficients ( $c$ ,  
 125  $c_i, l_j, o_k$ ). The first row represents the numerator and will only contain a single non-zero value.  
 126 The second row then represents the denominator. Storing the equations this way ensures we can  
 127 efficiently substitute in parameter values by taking the dot product with a vector representing a  
 128 point in parameter space ( $\kappa_i, \lambda_j, \omega_k$ ) once the Laplace transform needs to be evaluated. Also, storing  
 129 equation coefficients in array form allows us to efficiently perform operations on the equations (see  
 130 2.1.3). A minimal representation of the GF therefore consists of an array containing all unique  
 131 equations, and an array of arrays with equation indices describing all paths through the graph.

### 132 2.1.3 discrete events

133 For the general description of the GF we have assumed that all competing processes have expo-  
 134 nentially distributed waiting times. It is possible however to incorporate events that only happen

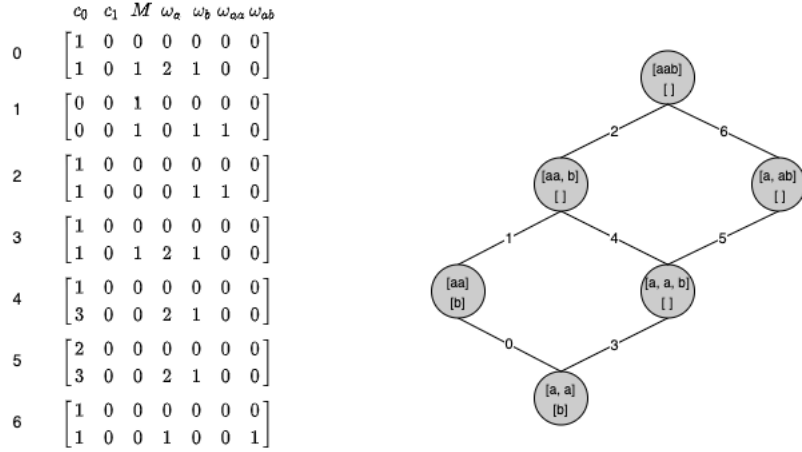


Figure 1: **From coalescent state space to equation array:** coalescent state space graph for two populations  $A$  and  $B$  with 2 and 1 unphased sample(s) respectively. The demographic model assumes a single mass migration event from population  $B$  to  $A$  back in time.

once. Initially treating these discrete events as a competing exponential process with rate  $\delta$ , we can recover the GF parametrised by the discrete time  $T$  of the event, by taking the inverse transform of the GF divided by its associated dummy variable ( $\delta$ ). This has been used to incorporate population splits and bottlenecks (Lohse et al., 2011; Bunnefeld et al., 2015) as well as hard sweeps (Bisschop et al., 2021).

Previous implementations have relied on a CAS to get an analytic solution for the inverse transform upon each evaluation of the GF. However, it is clearly overkill to determine the inverse Laplace symbolically repeatedly given that the GF will always be a sum of products of factors of the form  $c/(d + \delta)$  with  $c$  and  $d$  constants, independent of the complexity of the state space graph. That is, at least as long as we limit ourselves to a single discrete event. Having stored all equation coefficients as an array, we can formulate a closed-form solution to the inverse Laplace that allows for efficient substitution of all parameter values (see S3).

If we want to maintain the outlined correspondence between the state space graph and the GF as a sum of the products of the expressions associated with each path then we have to modify the state space graph. This can be done by creating a new node for each section of all paths leading up to a node associated with a discrete event. Each of these new nodes is connected to the root of the graph by a single edge associated with its respective inverse (see fig. 2.1.3).

In essence this means that the part of the path downstream of the discrete event remains

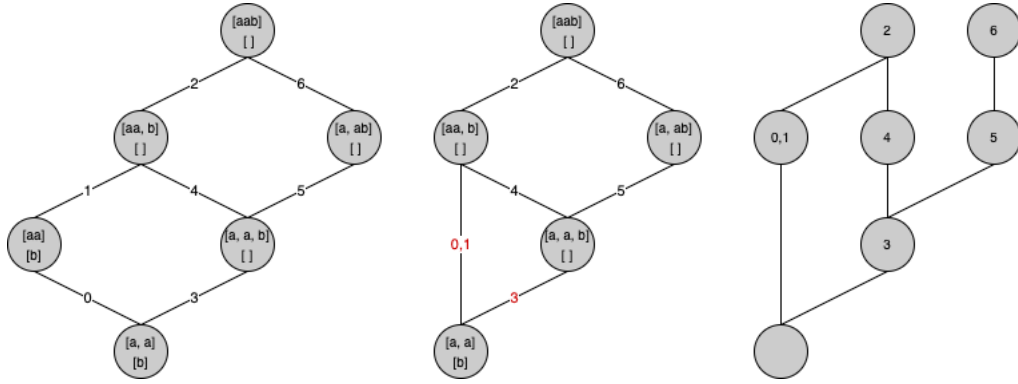


Figure 2: **From coalescent state space to equation graph:** setup identical as fig. 2.1.2. A shows the initial coalescent state space graph, while B shows the collapsed form grouping all parts of each path that require inverting with respect to the dummy variable associated with the discrete event. C takes this logic one step further turning the (sets of) equations previously associated with the edges into nodes, simplifying algorithms that do not require state space information.

unaltered, each edge still associated with a simple equation of the form 1. While each path upstream of that node is now collapsed into a single node. Once this operation has been performed, each path of the graph represents a product of factors again. Under the hood however, we perform a graph inversion while collapsing turning edges into nodes and vice versa (see fig. 2.1.3 C). This simplifies the graph traversal algorithm (see 2.2).

#### 2.1.4 adding new events

Currently, besides coalescence, two types of events have been implemented: uni-directional migration at a constant rate and population splits (forwards in time). Other events can readily be incorporated by adding in a method that provides a description of what the event does to the configuration of lineages (or node label) while generating the state space graph. There are two limitations however. First of all, the defined events should not lead to cycles in the directed graph. For example, in line with Lohse et al. (2016) migration is limited to being uni-directional such that lineages cannot cycle indefinitely between populations without ever reaching the fully coalesced state. Finally, note that so far our approach is only compatible with a single discrete event. Adding in more discrete events would require the use of a CAS to determine the inverse transform.

## 2.2 graph traversal

Given an equation graph (as described in 2.1.3) and a dependency sequence describing the evaluation order of the graph, a general algorithm to propagate any evaluation of the equations associated with each node is given by alg. 1. It relies on the fact that implicitly the edges of the graph represent multiplication. Once both multiplication and addition have been defined for the propagated values we can rely on the commutative property to efficiently traverse the graph towards the root. Especially in the case where addition is a less costly operation than multiplication (as is the case for polynomials, see 2.3), it will pay off to add the values associated with the children of a node prior to multiplication. We can now apply this algorithm to efficiently calculate the bSFS.

---

**Algorithm 1:** Propagate values through graph.

---

```

1 function PROPAGATE;
   Input: adjacency list of graph, node_values, evaluation_order
2 foreach parent in evaluation_order do
3   children = graph[parent];
4   temp = 0;
5   if children then
6     foreach child in children do
7       temp += node_values[child];
8     end
9     if parent not root then
10      node_values[parent] = PRODUCT(temp, node_values[parent]);
11    else
12      return temp;
13    end
14  end
15 end

```

---

## 2.3 blockwise site frequency spectrum

### 2.3.1 graph traversal

The block-wise site frequency spectrum or bSFS is the vector of site frequency spectrum counts in short blocks of a fixed length (Bunnefeld et al., 2015). It is the probability of seeing  $k_i$  mutations on each of the  $i$  distinguished branchtypes. For an unphased sample of size 3 the bSFS would be



182 a vector of the form  $\{k_1, k_2\}$  with  $k_1$  and  $k_2$  representing the number of singletons and doubletons  
 183 respectively. Each count is an element within the interval  $[0, 1, 2, \dots, k_i^{max} + 1]$  where  $k_i^{max} + 1$  is  
 184 used to bin all mutation configurations with more than  $k_i^{max}$  mutations.

185 Deriving the probability for each of the  $(\prod_{i=1}^c k_i^{max} + 2)$  possible bSFS configurations, with  $c$   
 186 the length of the bSFS vector, has thus far been the way in which the recursively generated Laplace  
 187 transform of coalescence time distributions has been used. The probability of observing mutation  
 188 configuration  $\mathbf{k}$  under a specified model can be obtained by taking the  $k_i^{\text{th}}$  derivative with respect  
 189 to  $\omega_i$  (see eq. (1) in Lohse et al. (2011) for details).

190 Any naive approach, based on calculating all higher order derivatives using a CAS, will suffer  
 191 from an explosion in the number of terms due to the Leibniz or product rule when differentiating.  
 192 Generally a CAS will fail to take into account the fact that the same partial derivatives are computed  
 193 multiple times. This problem has been well-studied for the purpose of automatic differentiation  
 194 algorithms (Neidinger, 1992, 1995; Griewank et al., 2000; Bettencourt et al., 2019). One possible  
 195 approach to overcome this issue consists of implementing recurrence relations on how to build  
 196 and combine the coefficients of truncated Taylor series. For such a series, the coefficient of  $x^{\mathbf{k}}$   
 197 is indeed proportionate to the desired partial derivative. By defining the series coefficients for  
 198 all elementary functions and defining the recurrence relations for arithmetic operators as well as  
 199 function compositions one can build higher-order derivatives from the ground up while avoiding  
 200 having to recalculate the same derivative multiple times (Neidinger, 2013).

201 Translating this to the graph traversal algorithm outlined above requires us to first obtain all  
 202 coefficients for a truncated Taylor series of the equation associated with each node in the equation  
 203 graph. We can then use the algorithm defining the product of two truncated Taylor series (see alg.  
 204 (8) in Neidinger (2013) and alg. 2) to propagate the coefficients of the series associated with each  
 205 node. Note that adding two truncated Taylor series simply amounts to the pairwise addition of all  
 206 corresponding coefficients. To get at the higher order derivatives needed for the first step, we could  
 207 use the recurrence relations as defined in Neidinger (2013). However, all equations associated with  
 208 each of the nodes of the equation graph are well characterised. They fall into one of two categories  
 209 depending on whether an inversion step was needed. For each of the two categories we can define  
 210 a closed-form implementation of the derivatives with respect to the distinguished branchtypes (see  
 211 eqs. S1 and S2).

212 Remark that alg. 2 contains an explicit ADD function. Care needs to be taken when summing  
 213 (a subset of) the coefficients of a Taylor series. These will be both positive and negative, and as  
 214 such catastrophic cancellation might occur leading to accuracy loss. The compensated summation  
 215 algorithm of Ogita-Rump-Oishi (Ogita et al., 2005) is implemented as an efficient way to bound the  
 216 potential loss in accuracy. Another way of handling this would be to temporarily increase numeric  
 217 precision at the crucial steps. Lastly, an advantage of using Taylor series coefficients rather than

---

**Algorithm 2:** Product of two truncated Taylor series (Neidinger, 2013).

---

```
1 function SERIES_PRODUCT;  
   Input  : Two same-size arrays of floats  $a$  and  $b$   
   Output: array  $c$  of same size as  $a$  and  $b$   
2 foreach multi-index  $\mathbf{k}$  do  
3    $sum = 0$ ;  
4   foreach multi-index  $\mathbf{j} \leq \mathbf{k}$  do  
5      $sum = \text{ADD}(sum, a[\mathbf{j}] * b[\mathbf{k} - \mathbf{j}])$ ;  
6   end  
7    $c[\mathbf{k}] = sum$ ;  
8 end  
9 return  $c$  [ ];
```

---

218 the derivatives is that the coefficients will always be smaller by a factor  $(\sum \mathbf{k})!$  leading to less  
219 cumulative roundoff error.

### 220 2.3.2 Mutation type equivalences

221 When labelling each branch by the labels of the lineages it subtends, the number of branch types  
222 and therefor the number of mutation types (a single bSFS vector), will quickly go up. Calculating  
223 the probability for observing each one of these will quickly become unfeasible. To alleviate this we  
224 can make two types of simplifications. Following Lohse et al. (2016), we can remove phase and/or  
225 root information by a relabelling of the branches. This reduces the number of branch types and  
226 mutation types one distinguishes. Phase is removed by labelling all branches according to their  
227 number of descendants in each subpopulation. Root information on the other hand can be left out  
228 by giving all branches the same label as the branches subtending the complement of that set of  
229 samples subtended by the first. Note that applying these simplifications might mean one cannot  
230 fully use all information present in a dataset. On the other hand, to date many datasets do not  
231 contain phase and/or root information.

232 Additionally, we can make use of the fact that some mutation types are inherently equiprobable.  
233 For example, given a sample from a single population labelled  $\{\{a, b, c\}\}$  mutation type  $\{a, ab\}$  will  
234 have the same probability as 5 other mutation types. To determine this equivalence it suffices to  
235 see that each mutation type can be represented in two ways. Either each mutation type is labelled  
236 as an integer vector indicating presence or absence of one or more mutations along branch types  
237  $\{a, b, c, ab, ac, bc\}$ . In our example this equates to  $\{1, 0, 0, 1, 0, 0\}$ . Similarly, each branch type can

238 be represented as an integer vector  $a, b, c$  indicating the lineages subtended by that branch. And  
 239 because all mutation types are labelled by the branches along which we observe a mutation, each  
 240 mutation type can also be represented by an array where each row is the integer vector representing  
 241 those branch types. For our example, this becomes:

$$\begin{array}{ccc} 1 & 0 & 0 \\ 1 & 1 & 0 \end{array}$$

242 In this representation, all permutations of columns representing samples from the same population  
 243 represent equiprobable configurations.

244 Besides all this, a large fraction of mutation types is simply impossible to observe. Realising  
 245 that the bSFS is a sparse array can reduce computation time even further by limiting computation  
 246 to those mutation types that can actually be observed.

### 247 3 Results and Discussion

248 The work presented here constitutes a CAS-independent, open-source implementation of the GF  
 249 approach. A general outline has been given on how to rely on the correspondence between the coa-  
 250 lescent state space graph and the GF to query the distribution of Laplace transformed coalescence  
 251 times efficiently. In particular, an algorithm has been laid out to efficiently calculate the bSFS  
 252 making this package ideal as a backend for likelihood calculations.

253 To quantify the speedup of the new algorithm, we compare its performance against the original  
 254 implementation (Lohse et al., 2011) as well as against a simulation-based approach as described in  
 255 Beeravolu et al. (2018). Using `msprime` (Baumdicker et al., 2021) coalescent trees can be simulated  
 256 under (almost) any demographic model. Without having to simulate mutations we can calculate  
 257 the probability for each of the distinguished mutation types. Given that mutations on each branch  
 258 type happen independently, the probability of seeing mutation configuration  $(k_1, k_2, \dots, k_n)$  is given  
 259 by the product of  $n$  probabilities as given by a Poisson distribution with rate  $\theta * t_i$ . Here,  $t_i$  is the  
 260 total branch length of branch type  $i$  and  $\theta = 2N_e\mu$ . When averaged across many replicates the  
 261 true value will be approximated. Note that particular entries of the bSFS might require fewer/more  
 262 replicates to get at a good approximation than others (Beeravolu et al., 2018). Fig ?? shows ...

263 Currently, `agemo` is implemented in `python 3`, relying on `numba` just-in-time compilation to  
 264 speed up the critical parts of the code. Compiling the code using `numba` has a few consequences.  
 265 Firstly, compilation happens each time the code is run and will require a few seconds. This is  
 266 generally not an issue given that usually for a single model many points in parameter space will  
 267 be evaluated. Secondly, some numerical operations are implemented differently in `numba` than  
 268 in `numpy`. In the case of summation this can lead to a loss of precision and has required us to

269 implement a compensated sum algorithm. A potentially faster solution would be to temporarily  
 270 increase machine precision for the evaluation of particular sums. This is not possible using `numba`  
 271 however and would require us to transfer part of the code to `C`.

272 There are more efficient algorithms to multiply (truncated) multivariate polynomials. The fast  
 273 Fourier transform (FFT) would allow us to perform the operation at  $\mathcal{O}(n \log(n))$  with  $n$  the order  
 274 of the polynomial instead of  $\mathcal{O}(n^2)$  for the current multiplication. However, gains would only be  
 275 noticeable for a large number of distinguished branch types, or a really large  $k_{max}$  value.

276  
 277 As indicated in the methods section, extending the GF approach by defining a new type of  
 278 event can easily be done. Because of its recursive nature, it only requires defining a function that  
 279 describes the impact of the event on the extant lineages. However, even though we can recursively  
 280 generate the expression associated with a model that includes multiple discrete events, retrieving the  
 281 expression parametrised by the time to each of those events requires taking an inverse Laplace with  
 282 respect to the dummy variable describing the event. Taking multiple inverse Laplace transforms  
 283 can become prohibitively difficult for large expressions, even when performed symbolically. Because  
 284 of this, the current implementation only contains closed-form expressions to efficiently evaluate the  
 285 GF associated with a single discrete event (and none, one or more non-discrete events).

286 Although most people still process vcfs when it comes to mutation data. There is the more  
 287 succinct treesequences format containing both topology information as well as mutations. It would  
 288 therefore make a lot of sense to add on the ability to calculate the likelihood of a mutation config-  
 289 uration under a particular coalescent model as given by a marginal tree from a treesequences. This  
 290 boils down to restricting the GF for that particular model to the observed topology, counting the  
 291 number of mutations of each distinguished branch type and computing its probability. Note though  
 292 that inferred tree sequences might contain polytomies that won't have a one-to-one correspondence  
 293 to any binary tree topology.

294 Even though this work was motivated by finding an efficient way to get out the bSFS, this is not  
 295 the only way to use the GF. In line with restricting the GF to particular topologies, `agemo` could  
 296 easily be extended to get at the probability of seeing a particular topology under any structured  
 297 coalescent model. Taking one step back, one might not even have to resort to evaluating the GF to  
 298 get at the distribution of certain statistics. A model fit could be performed on the empirical Laplace  
 299 transformed distribution of coalescence times as implemented in `MAGIC` (Weissman and Hallatschek,  
 300 2017).

301 The algorithm described in this paper will not suddenly make it possible to extent the usage  
 302 of the GF to any arbitrary model and sample size. The fact remains that the number of sample  
 303 configurations grows super-exponentially with sample size (Lohse et al., 2016). At some point  
 304 complex models will be easier to simulate (and extract the bSFS from) rather than using the GF

approach. However, this paper demonstrates that the Laplace transform as a mathematical object can simplify the description of a problem allowing us to come up with efficient algorithms to evaluate these expressions computationally. As such, this paper paves the way for all future work on the joint distribution of branch lengths using generating functions.

## acknowledgements

This work was supported by an ERC starting grant (ModelGenomLand, 757648)

## References

- Barton, N. H. and Wilson, I. (1995). Genealogies and geography. *Philosophical Transactions of the Royal Society B*, 349(1327):49–59.
- Baumdicker, F., Bisschop, G., Goldstein, D., Gower, G., Ragsdale, A. P., Tsambos, G., Zhu, S., Eldon, B., Ellerman, C. E., Galloway, J. G., Gladstein, A. L., Gorjanc, G., Guo, B., Jeffery, B., Kretzschmar, W. W., Lohse, K., Matschiner, M., Nelson, D., Pope, N. S., Quinto-Cortés, C. D., Rodrigues, M. F., Saunack, K., Sellinger, T., Thornton, K., van Kemenade, H., Wohns, A. W., Wong, H. Y., Gravel, S., Kern, A. D., Koskela, J., Ralph, P. L., and Kelleher, J. (2021). Efficient ancestry and mutation simulation with msprime 1.0. *bioRxiv*.
- Beeravolu, C. R., Hickerson, M. J., Frantz, L. A. F., and Lohse, K. (2018). ABLE: blockwise site frequency spectra for inferring complex population histories and recombination. *Genome Biology*, 19(1):145.
- Bettencourt, J., Johnson, M. J., and Duvenaud, B. D. (2019). Taylor-Mode Automatic Differentiation for Higher-Order Derivatives in JAX. 10.
- Bisschop, G., Lohse, K., and Setter, D. (2021). Sweeps in time: Leveraging the joint distribution of branch lengths. *Genetics*, 219(2).
- Bunnefeld, L., Frantz, L. A., and Lohse, K. (2015). Inferring bottlenecks from genome-wide samples of short sequence blocks. *Genetics*, 201(3):1157–1169.
- Excoffier, L., Dupanloup, I., Huerta-Sánchez, E., Sousa, V. C., and Foll, M. (2013). Robust Demographic Inference from Genomic and SNP Data. *PLoS Genetics*, 9(10).
- Griewank, A., Utke, J., and Walther, A. (2000). Evaluating Higher Derivative Tensors by Forward Propagation of Univariate Taylor Series Source : Mathematics of Computation , Jul ., 2000 , Vol . 69 , No . 231 ( Jul ., 2000 ), pp . 1117- Publi. *Mathematics of Computation*, 69(231):1117–1130.

334 Griffiths, R. C. (1991). The Two-Locus Ancestral Graph. *Selected proceedings of the Sheffield*  
335 *symposium on applied probability*, 18(1991):100–117.

336 Gutenkunst, R. N., Hernandez, R. D., Williamson, S. H., and Bustamante, C. D. (2009). Inferring  
337 the Joint Demographic History of Multiple Populations from Multidimensional SNP Frequency  
338 Data. *PLoS Genetics*, 5(10):e1000695.

339 Hey, J. (2004). Multilocus Methods for Estimating Population Sizes, Migration Rates and Diver-  
340 gence Time, With Applications to the Divergence of *Drosophila pseudoobscura* and *D. persimilis*.  
341 *Genetics*, 167(2):747–760.

342 Hobolth, A., Siri-Jégousse, A., and Bladt, M. (2019). Phase-type distributions in population ge-  
343 netics. *Theoretical Population Biology*, 127:16–32.

344 Hudson, R. R. (1983). Testing the constant-rate neutral allele model with protein sequence data.  
345 *Evolution*, 37(1):203–217.

346 Kingman, J. F. (1982). The coalescent. *Stochastic Processes and their Applications*, 13(3):235–248.

347 Lohse, K., Chmelik, M., Martin, S. H., and Barton, N. H. (2016). Efficient strategies for calculating  
348 blockwise likelihoods under the coalescent. *Genetics*, 202(2):775–786.

349 Lohse, K., Harrison, R. J., and Barton, N. H. (2011). A general method for calculating likelihoods  
350 under the coalescent process. *Genetics*, 189(3):977–987.

351 Neidinger, R. D. (1992). An Efficient Method for the Numerical Evaluation of Partial Derivatives  
352 of Arbitrary Order. *ACM Transactions on Mathematical Software (TOMS)*, 18(2):159–173.

353 Neidinger, R. D. (1995). Computing multivariable Taylor series to arbitrary order. In *Proceedings*  
354 *of the international conference on Applied programming languages - APL '95*, pages 134–144,  
355 New York, New York, USA. ACM Press.

356 Neidinger, R. D. (2013). Efficient recurrence relations for univariate and multivariate Taylor series  
357 coefficients. *Conference Publications*, pages 587–596.

358 Nielsen, R. and Wakeley, J. (2001). Distinguishing migration from isolation: A Markov chain Monte  
359 Carlo approach. *Genetics*, 158(2):885–896.

360 Notohara, M. (1990). The coalescent and the genealogical process in geographically structured  
361 population. *Journal of mathematical biology*, 29:59–75.

362 Ogita, T., Rump, S. M., and Oishi, S. (2005). Accurate sum and dot product. *SIAM Journal on*  
363 *Scientific Computing*, 26(6):1955–1988.

- 364 Råde, L. (1972). On the use of generating functions and laplace transforms in applied probability  
365 theory. *International Journal of Mathematical Education in Science and Technology*, 3(1):25–33.
- 366 Tajima, F. (1983). Evolutionary relationship of DNA sequences in finite populations. *Genetics*,  
367 105(2):437–460.
- 368 Takahata, N. (1988). The coalescent in two partially isolated diffusion populations. *Genetical*  
369 *Research*, 52(3):213–222.
- 370 Weissman, D. B. and Hallatschek, O. (2017). Minimal-assumption inference from population-  
371 genomic data. *eLife*, 6:1–21.
- 372 Wilkinson-Herbots, H. M. (1998). Genealogy and subpopulation differentiation under various mod-  
373 els of population structure. *Journal of Mathematical Biology*, 37(6):535–585.
- 374 Yang, Z. (2002). Likelihood and Bayes estimation of ancestral population sizes in hominoids using  
375 data from multiple loci. *Genetics*, 162(4):1811–1823.

## 376 **Supplementary Information**

### 377 **closed-form derivatives**

378 Given a first degree multivariate polynomial of the form  $f(\mathbf{x}) = \sum c_i x_i + b$ , then the following  
 379 higher order derivatives have a closed form. With  $s = \sum k_i$

$$\frac{\partial f(\mathbf{x})^{-1}}{\partial^{k_i} x_i} = (-1)^s s! \frac{c_i^{k_i}}{f(\mathbf{x})^2} \quad (\text{S1})$$

$$\frac{\partial e^{cf(\mathbf{x})}}{\partial^{k_i} x_i} = c^s c_i^{k_i} e^{cf(\mathbf{x})} \quad (\text{S2})$$

380 These two base case derivatives together with the defined Taylor series product allow us to calculate  
 381 all required derivatives for the entire GF assuming at most only a single inverse Laplace with respect  
 382 to a discrete event is required.

### 383 **closed-form inverse Laplace transform**

384 Given  $f(c) = \frac{1}{c+\delta}$ , the inverse Laplace transforms (wrt  $\delta$ ) can be defined as follows. Here  $T$   
 385 represents the time to the discrete event.

$$g(T) = \mathcal{L}^{-1}\left(\frac{1}{\prod_{i=0} f_i(\mathbf{x})}\right) = \sum_i \frac{(-1)^{i+1} e^{-cT}}{\prod_{i \neq j} (f_{\min(i,j)}(\mathbf{x}) - f_{\max(i,j)}(\mathbf{x}))} \quad (\text{S3})$$

386 Note that all derivatives of S3 can be determined using the equations from the section above.